# Net-gain from a parametric amplifier on a chalcogenide optical chip

**Michael R.E. Lamont,[1] Barry Luther-Davies,[2] Duk-Yong Choi,[2] Steve Madden,[2] Xin Gai[2] and Benjamin J. Eggleton[1]**

[1]*Centre for Ultrahigh-bandwidth Devices for Optical Systems (CUDOS), School of Physics, University of Sydney, NSW 2006, Australia*
egg@physics.usyd.edu.au
[2]*Centre for Ultrahigh-bandwidth Devices for Optical Systems (CUDOS), Laser Physics Centre, The Australian National University, Canberra, ACT 0200, Australia*
bld111@rsphysse.anu.edu.au

**Abstract:** We report first observation of net-gain from an optical parametric amplifier in a planar waveguide. This was achieved in a low-loss $As_2S_3$ planar waveguide, with a strong nonlinearity ($\gamma \sim 10$ /W/m) and tailored anomalous dispersion yielding efficient Raman-assisted four-wave mixing at telecom wavelengths. The experiments were in good agreement with theory, and indicate a peak net-gain greater than +16 dB for the signal and idler (+30 dB neglecting coupling losses) and a broad bandwidth spanning 180 nm.



**OCIS codes:** (190.4380) Nonlinear optics, four-wave mixing; (190.4970) Parametric oscillators and amplifiers; (230.7390) Waveguides, planar.

## References and links

1. M. E. Marhic, N. Kagi, T. K. Chiang, and L. G. Kazovsky, "Broadband fiber optical parametric amplifiers," Opt. Lett. **21**, 573-575 (1996).
2. C. J. McKinstrie, S. Radic, and A. R. Chraplyvy, "Parametric amplifiers driven by two pump waves," IEEE J. Sel. Top. Quantum Electron. **8**, 538-547 (2002).
3. S. Radic, C. J. McKinstrie, A. R. Chraplyvy, G. Raybon, J. C. Centanni, C. G. Jorgensen, K. Brar, and C. Headley, "Continuous-wave parametric gain synthesis using nondegenerate pump four-wave mixing," IEEE Photon. Technol. Lett. **14**, 1406-1408 (2002).
4. M. Hirano, T. Nakanishi, T. Okuno, and M. Onishi, "Broadband wavelength conversion over 193-nm by HNL-DSF improving higher-order dispersion performance," in *European Conference on Optical Communication* (Glasgow, Scotland, 2005), paper Th4.4.4.
5. M. E. Marhic, Y. Park, F. S. Yang, and L. G. Kazovsky, "Broadband fiber-optical parametric amplifiers and wavelength converters with low-ripple Chebyshev gain spectra," Opt. Lett. **21**, 1354-1356 (1996).
6. E. Ciaramella, and S. Trillo, "All-optical signal reshaping via four-wave mixing in optical fibers," IEEE Photon. Technol. Lett. **12**, 849-851 (2000).
7. S. Radic, C. J. McKinstrie, R. M. Jopson, J. C. C. A.-J. C. Centanni, and A. R. C. A.-A. R. Chraplyvy, "All-optical regeneration in one- and two-pump parametric amplifiers using highly nonlinear optical fiber," IEEE Photon. Technol. Lett. **15**, 957-959 (2003).
8. R. Salem, M. A. Foster, A. C. Turner, D. F. Geraghty, M. Lipson, and A. L. Gaeta, "Signal regeneration using low-power four-wave mixing on silicon chip," Nat. Photonics **2**, 35-38 (2008).
9. S. Watanabe, and M. Shirasaki, "Exact compensation for both chromatic dispersion and Kerr effect in a transmission fiber using optical phase conjugation," J. Lightwave Technol. **14**, 243-248 (1996).
10. A. Yariv, D. Fekete, and D. M. Pepper, "Compensation for channel dispersion by nonlinear optical phase conjugation," Opt. Lett. **4**, 52 (1979).
11. M. A. Foster, A. C. Turner, J. E. Sharping, B. S. Schmidt, M. Lipson, and A. L. Gaeta, "Broad-band optical parametric gain on a silicon photonic chip," Nature **441**, 960-963 (2006).
12. H. Fukuda, K. Yamada, T. Shoji, M. Takahashi, T. Tsuchizawa, T. Watanabe, J.-i. Takahashi, and S.-i. Itabashi, "Four-wave mixing in silicon wire waveguides," Opt. Express **13**, 4629-4637 (2005).
13. M. Asobe, T. Kanamori, K. Naganuma, H. Itoh, and T. Kaino, "Third-Order Nonlinear Spectroscopy in $As_2S_3$ Chalcogenide Glass-Fibers," J. Appl. Phys. **77**, 5518-5523 (1995).
14. M. R. E. Lamont, C. M. de Sterke, and B. J. Eggleton, "Dispersion engineering of highly nonlinear $As_2S_3$ waveguides for parametric gain and wavelength conversion," Opt. Express **15**, 9458-9463 (2007).

#103490 - $15.00 USD Received 31 Oct 2008; revised 20 Nov 2008; accepted 21 Nov 2008; published 24 Nov 2008

15. Q. Lin, J. D. Zhang, P. M. Fauchet, and G. P. Agrawal, "Ultrabroadband parametric generation and wavelength conversion in silicon waveguides," Opt. Express **14**, 4786-4799 (2006).
16. J. Meier, W. S. Mohammed, A. Jugessur, L. Qian, M. Mojahedi, and J. S. Aitchison, "Group velocity inversion in AlGaAs nanowires," Opt. Express **15**, 12755-12762 (2007).
17. A. C. Turner, C. Manolatou, B. S. Schmidt, M. Lipson, M. A. Foster, J. E. Sharping, and A. L. Gaeta, "Tailored anomalous group-velocity dispersion in silicon channel waveguides," Opt. Express **14**, 4357-4362 (2006).
18. I. W. Hsieh, X. G. Chen, X. P. Liu, J. I. Dadap, N. C. Panoiu, C. Y. Chou, F. N. Xia, W. M. Green, Y. A. Vlasov, and R. M. Osgood, "Supercontinuum generation in silicon photonic wires," Opt. Express **15**, 15242-15249 (2007).
19. M. R. E. Lamont, B. Luther-Davies, D.-Y. Choi, S. Madden, and B. J. Eggleton, "Supercontinuum generation in dispersion engineered highly nonlinear ($\gamma$ = 10 /W/m) $As_2S_3$ chalcogenide planar waveguide," Opt. Express **16**, 14938-14944 (2008).
20. G. P. Agrawal, *Nonlinear Fiber Optics* (Academic Press, San Diego, California, 2001).
21. J. S. Browder, S. S. Ballard, and P. Klocek, "Physical properties of glass infrared optical materials," in *Handbook of infrared optical materials*, P. Klocek, ed. (Marcel Dekker, Inc., New York, New York, 1991).
22. S. J. Madden, D. Y. Choi, D. A. Bulla, A. V. Rode, B. Luther-Davies, V. G. Ta'eed, M. D. Pelusi, and B. J. Eggleton, "Long, low loss etched $As_2S_3$ chalcogenide waveguides for all-optical signal regeneration," Opt. Express **15**, 14414-14421 (2007).
23. D. Y. Choi, S. Madden, A. Rode, R. P. Wang, and B. Luther-Davies, "Plasma etching of $As_2S_3$ films for optical waveguides," J. Non-Cryst. Solids **354**, 3179-3183 (2008).
24. O. V. Sinkin, R. Holzlohner, J. Zweck, and C. R. Menyuk, "Optimization of the split-step Fourier method in modeling optical-fiber communications systems," J. Lightwave Technol. **21**, 61-68 (2003).
25. M. C. Ho, K. Uesaka, M. Marhic, Y. Akasaka, and L. G. Kazovsky, "200-nm-bandwidth fiber optical amplifier combining parametric and raman gain," J. Lightwave Technol. **19**, 977-981 (2001).
26. T. Torounidis, and P. Andrekson, "Broadband single-pumped fiber-optic parametric amplifiers," IEEE Photon. Technol. Lett. **19**, 650-652 (2007).
27. T. Shoji, T. Tsuchizawa, T. Watanabe, K. Yamada, and H. Morita, "Low loss mode size converter from 0.3 mu m square Si wire waveguides to singlemode fibres," Electron. Lett. **38**, 1669-1670 (2002).
28. V. G. Ta'eed, M. D. Pelusi, B. J. Eggleton, D. Y. Choi, S. Madden, D. Bulla, and B. Luther-Davies, "Broadband wavelength conversion at 40 Gb/s using long serpentine As2S3 planar waveguides," Opt. Express **15**, 15047-15052 (2007).
29. A. S. Y. Hsieh, G. K. L. Wong, S. G. Murdoch, S. Coen, F. Vanholsbeeck, R. Leonhardt, and J. D. Harvey, "Combined effect of Raman and parametric gain on single-pump parametric amplifiers," Opt. Express **15**, 8104-8114 (2007).

## 1. Introduction

The wavelength range available to current telecommunication networks is limited primarily by the gain spectrum of erbium-doped fiber amplifiers (EDFA). Because of this, only a fraction of the possible bandwidth available to fiber optic networks is useable; and this frequency range is inflexible, set by the properties of the erbium atom. Optical parametric amplifiers (OPAs) using nonlinear processes such as four-wave mixing (FWM) do not have such limitations, they can amplify over broader bandwidths and the amplified frequency range can be altered by adjusting the pump frequency [1, 2]. OPAs have the potential to increase the efficiency of current fiber optic networks by expanding it into new wavelengths. As well as amplification [3], FWM can be used for wavelength conversion [4, 5], optical regeneration [6-8] and the reversal of signal impairments through optical phase conjugation [9, 10].

Planar waveguides made from nonlinear materials such as silicon make it possible to integrate FWM-based amplifiers and wavelength converters onto optical chips [11, 12]. Although silicon has a high nonlinear refractive index, it also has high nonlinear losses due to two-photon absorption and free-carrier creation, which limit the maximum gain possible. The maximum parametric gain reported in silicon waveguides thus far is +1.8 dB, if coupling losses are not included (more than -12 dB per facet) [11]. Chalcogenide glasses, on the other hand, have a comparable nonlinear index, but much lower two-photon absorption and no free carriers [13]. Because of the strong confinement offered by a high refractive index, both materials can exploit waveguide dispersion to compensate for their normal material dispersions, and achieve anomalous dispersion at telecom wavelengths [14-17], allowing the phase-matching necessary for efficient FWM. With a transparency window from near-

#103490 - $15.00 USD Received 31 Oct 2008; revised 20 Nov 2008; accepted 21 Nov 2008; published 24 Nov 2008

infrared out to the mid-infrared, chalcogenide glasses can enable amplification over wide wavelength range.

Previously, we have used dispersion engineered $As_2S_3$ chalcogenide waveguides to demonstrate the benefits of chalcogenide's low nonlinear loss, in comparison to silicon waveguides, in the context of supercontinuum generation [18, 19]. Here we report the first observation of net-gain in an OPA on an optical chip using a similar $As_2S_3$ waveguide. Furthermore, the FWM gain peak occurs within the Raman gain spectrum, further enhancing the signal amplification. We achieved a broad gain bandwidth of over 180 nm and a peak gain more than +30 dB, including propagation losses. This can be compared to the best result in silicon waveguides, which has a bandwidth spanning 80 nm with a peak gain of +1.8 dB. If all coupling losses are considered, the device still has a large net gain of +18 dB. These results are in good agreement with presented theory and highlight chalcogenide as a platform for all-optical ultrahigh speed processing in a monolithic platform.

## 2. Background

As a parametric process, FWM is governed by a phase-matching condition. Specifically, degenerate four-wave mixing (D-FWM) uses a single pump such that, in the correct dispersive conditions, energy from the high-power pump wave (at an angular frequency $\omega_p$) is transferred at an exponential rate to a low-power signal wave (at $\omega_s$) and into the creation of an idler wave (at $\omega_i = 2\omega_p - \omega_s$), as illustrated in Fig. 1. The phase-matching condition depends on a dispersive-phase mismatch term, $\Delta\beta = \frac{1}{2}(\beta_s + \beta_i - 2\beta_p)$, where $\beta_x$ is the mode-propagation constant at $\omega_x$. The dispersive-phase mismatch must lie between $-2\gamma P_p < \Delta\beta < 0$ for exponential gain in the signal and idler [2, 20], where $\gamma$ is the nonlinear parameter of the waveguide and $P_p$ is the peak power of the pump. Thus for gain near $\omega_P$, the pump must experience anomalous dispersion.

Because $As_2S_3$ has a normal material dispersion, anomalous waveguide dispersion is introduced by reducing the transverse dimensions of the waveguide to "squeeze" the mode; the total dispersion is then the sum of the dispersion due to the material and due to the waveguide geometry. The dimensions of the $As_2S_3$ rib waveguide are shown in Fig. 2(a), with the fundamental quasi-TM (vertically polarized) mode field diagram in Fig. 2(b). A finite-element mode solver, FemSIM™, was used to calculate the dispersion of this fundamental mode, shown in Fig. 2(c), and was engineered to be anomalous at telecommunication wavelengths [14]. Figure 2(c) also shows the material dispersion of bulk $As_2S_3$ [21], the difference between the two curves being the result of waveguide dispersion. Therefore with a pump centered near 1550 nm, where $D$ = +30 ps/nm/km, we can expect to observe FWM gain

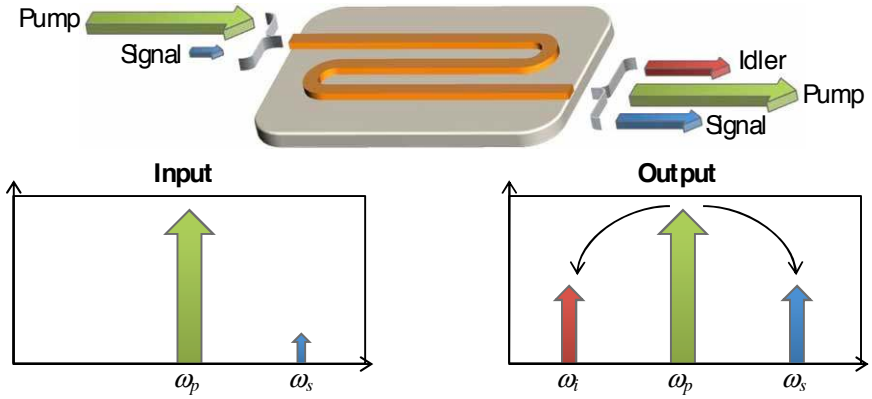


Fig. 1. Concept of single-pump (degenerate) four-wave mixing. A high-power pump and weak signal co-propagate within a nonlinear medium. If the phase-matching conditions are met, energy from the pump is transferred to the signal, providing amplification and creating an idler due to energy conservation. Note that the above shows a serpentine waveguide, whereas a straight waveguide is utilized in this paper.

#103490 - $15.00 USD Received 31 Oct 2008; revised 20 Nov 2008; accepted 21 Nov 2008; published 24 Nov 2008

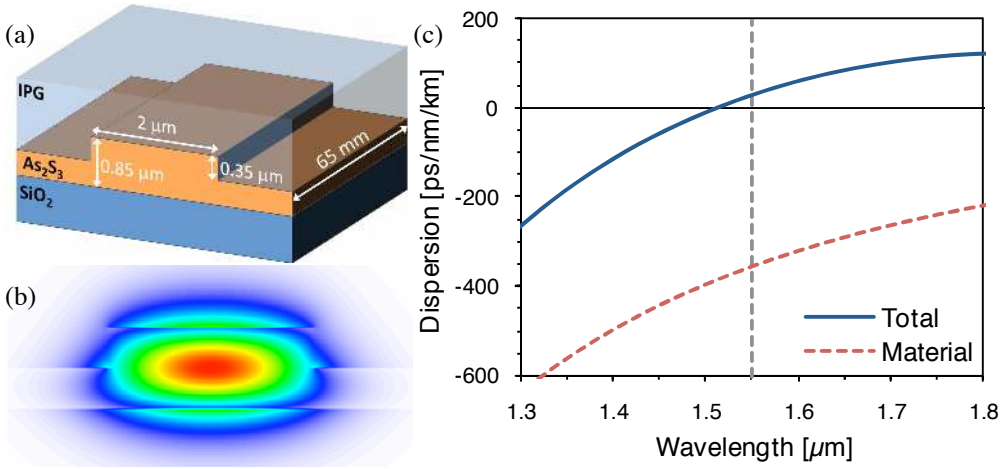


Fig. 2. (a) Schematic of the $As_2S_3$ rib waveguide. (b) The fundamental quasi-TM mode field. (c) Total and material dispersion curves for the waveguide shown in (a).

over a broad bandwidth. The effective area of this mode was calculated to be 1.2 $\mu m^2$ and, combined with a nonlinear refractive index $n_2$ of $3.0\times10^{-18}$ $m^2/W$, gave a nonlinear parameter $\gamma$ of ~9900 /W/km. This $\gamma$-value is slightly reduced due to the mode field extending beyond the nonlinear core, as shown in Fig. 2(b).

### 3. Experimental results

Figure 2(a) shows the basic geometry of the waveguide. $As_2S_3$ was deposited onto a silica-on-silicon substrate using thermal evaporation [22] to a thickness of 0.85 m. Photolithography was used to define 2 $\mu$m-wide waveguides and inductively coupled plasma reactive ion etching with $CHF_3$ gas was used to etch a 350nm deep rib waveguide [23]. The waveguide was 65 mm long and had a propagation loss estimated to be 0.5 dB/cm. Due to its high refractive index ($n \sim 2.4$), even at these small dimensions the waveguide supports two TE modes (horizontally polarized), although only one TM mode is expected. Only the fundamental TM mode is used in this experiment.

The experimental setup is shown in Fig. 3. To achieve a high peak power while maintaining a low average power, a low duty-cycle pulsed laser was used as the pump source. The pulsed pump was combined with a low-power CW signal using a 90/10 coupler. Input and output coupling to the $As_2S_3$ waveguide was achieved through lensed fibers, resulting in a loss of ~6.9 dB per facet including reflections. Polarization controllers (PC) were used to align the pump and signal independently to the TM-mode of the waveguide, and spectra were recorded using an optical spectrum analyzer (OSA). The 10 MHz mode-locked fiber laser provided pulses with a full-width at half-maximum of 3 ps at a wavelength of 1532 nm, and a coupled peak power of 9.6 W (39.8 dBm). The CW source had a coupled power of 0.032 mW (-14.9 dBm) and its wavelength was varied from 1550 to 1630 nm.

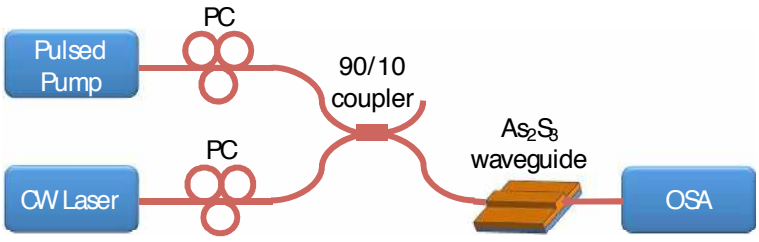


Fig. 3. Experimental setup used for measuring FWM spectra.

#103490 - $15.00 USD Received 31 Oct 2008; revised 20 Nov 2008; accepted 21 Nov 2008; published 24 Nov 2008

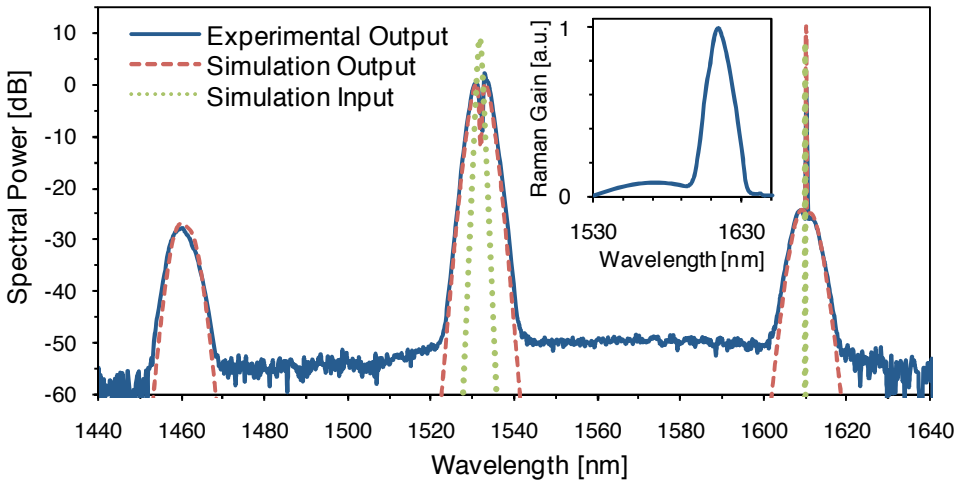


Fig. 4. Experimental spectrum (blue, solid line) after propagation through the $As_2S_3$ waveguide with the pump at 1532 nm and the CW signal at 1610 nm, compared to simulation (red, dashed line), with the simulated input spectrum (green, dotted line). The combined FWM and Raman gain estimated from simulation is +32.5 dB for the signal (from coupled input to output signal peak power) and +30.6 dB for the idler (from coupled input to output idler peak power). The inset shows the Raman gain spectrum, based on experimental measurement, used in the simulation.

The measured output spectrum indicating maximum gain is shown in Fig. 4 for the CW signal tuned to 1610 nm. The nonlinear Schrödinger equation (NLSE) [20] was used to calculate a numerical fit to the experimental spectrum;

$$\frac{\partial}{\partial z}A(z,t) = -\frac{\alpha}{2}A - i\frac{\beta_2}{2!}\frac{\partial^2 A}{\partial t^2} + \frac{\beta_3}{3!}\frac{\partial^3 A}{\partial t^3} + i\frac{\beta_4}{4!}\frac{\partial^4 A}{\partial t^4} + i\left(\gamma + i\frac{\alpha_2}{2A_{eff}}\right)\left(1 + \frac{i}{\omega_0}\frac{\partial}{\partial t}\right)\left(A(z,t)\int_{-\infty}^{\infty} R(t')\left|A(z,t-t')\right|^2 dt'\right), \quad (1)$$

where $A(z,t)$ is the electric field wave amplitude as a function of propagation distance and time, $\beta_n$ is the $n$-th order dispersion parameter; $\alpha$ is the linear loss; $\alpha_2$ is the two-photon absorption coefficient ($6.2\times10^{-15}$ m/W for $As_2S_3$); $A_{eff}$ is the effective area; $\omega_0$ is the average angular frequency; and $R(t) = (1\text{-}f_R)\delta(t) + f_R h_R(t)$ is the response function, including a Raman contribution $h_R(t)$ which was modeled using Raman gain spectrum measured experimentally in a similar $As_2S_3$ waveguide, with a fractional contribution of the delayed Raman response $f_R$ of 0.14. The NLSE was solved using the split-step Fourier method with an adaptive step-size algorithm [24]. The input field was constructed using the parameters given above and the dispersion described using the results shown in Fig. 2(c). The resulting simulated spectrum, also shown in Fig. 4, is in excellent agreement with the experimental spectrum. The output peak powers were calculated from the simulation to be 58 mW (17.7 dBm) for the signal and 37 mW (15.7 dBm) for the idler. This yields a signal gain (output signal to input signal peak power) of +32.5 dBm and an idler gain (output idler to input signal peak power) of +30.6 dBm. This is comparable to gain provided by EDFAs, or +15 to +25 dB of broadband parametric gain expected using tens of meters of highly nonlinear fiber (HNLF) and similar peak powers [25, 26], and far exceeds the +1.8 dB of net-gain achieved in silicon waveguides [11]. Even when coupling losses were included, the net gain was still large, at +18.8 dB for the signal and +16.8 dB for the idler. This is therefore the first time net-parametric gain has been observed in a planar waveguide.

#103490 - $15.00 USD Received 31 Oct 2008; revised 20 Nov 2008; accepted 21 Nov 2008; published 24 Nov 2008

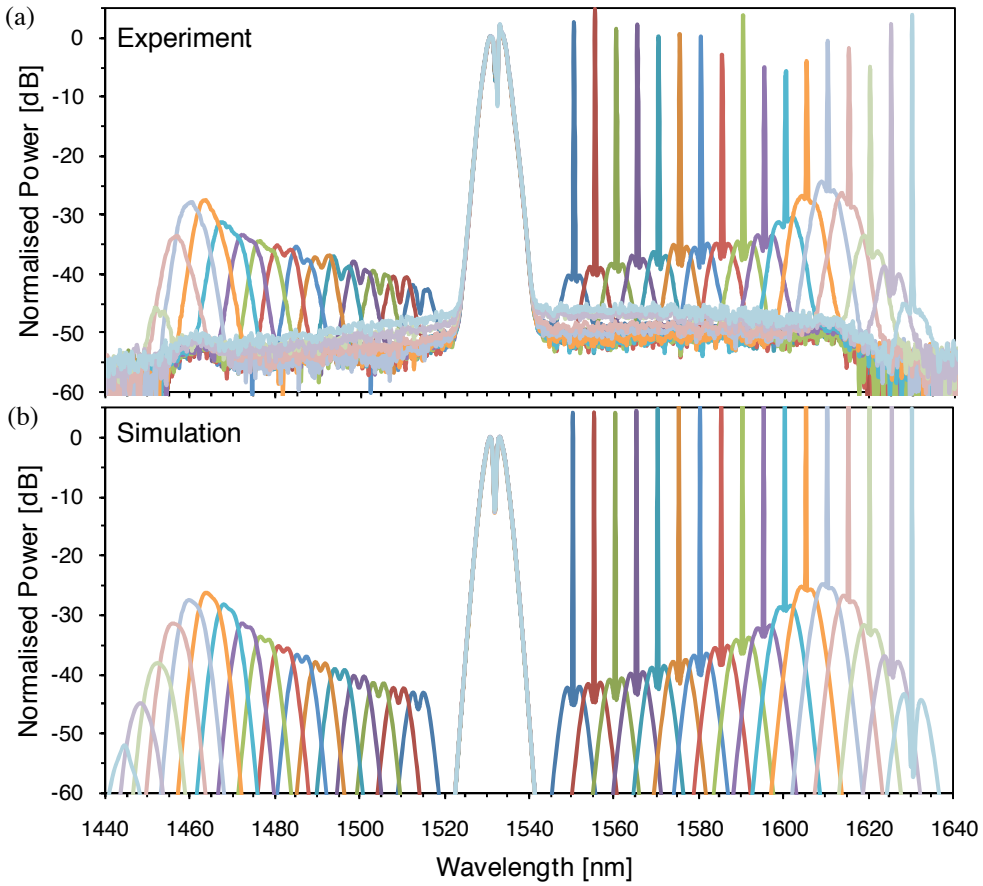


Fig. 5. (a) Experimental spectra after propagation through the $As_2S_3$ waveguide showing the FWM gain bandwidth with a pulsed pump at a wavelength of 1530 nm and a CW signal at wavelengths varying between 1550 nm and 1630 nm. (b) SSFM simulated spectra modeling the experiment using the dispersion shown in Fig. 2(c). Simulations suggest more than 30 dB of FWM gain (peak power in the idler compared to the signal input power) and a bandwidth of over 180 nm.

To investigate the bandwidth of the parametric gain, the CW signal wavelength was varied between 1550 and 1630 nm. The recorded spectra are shown in Fig. 5(a) and indicate a broad parametric gain bandwidth of 180 nm, spanning all of the C-band and most of the S- and L-bands as well. This is twice the bandwidth shown in silicon planar waveguides [11], and is similar to results demonstrated in HNLF [25]. The same simulation and parameters described previously were used to compare the experiment to theoretical expectations, shown in Fig. 5(b), again achieving excellent agreement.

## 4. Discussion and conclusion

The estimated signal and idler gain is shown in Fig. 6(a). The gain is calculated using the same simulation shown in Fig. 5(b), by filtering the spectrum and Fourier transforming this to find the peak power in the signal and idler. The horizontal lines indicates the level of gain needed to compensate for input and output coupling losses, i.e. any gain above this line is net-gain from the device. Again using the same simulation parameters, the gain dependence on pump power is illustrated in Fig. 6(b), showing a steady increase in signal and idler gain with increasing pump powers, with no sign of saturation. This contrasts with the case of silicon-

#103490 - $15.00 USD Received 31 Oct 2008; revised 20 Nov 2008; accepted 21 Nov 2008; published 24 Nov 2008

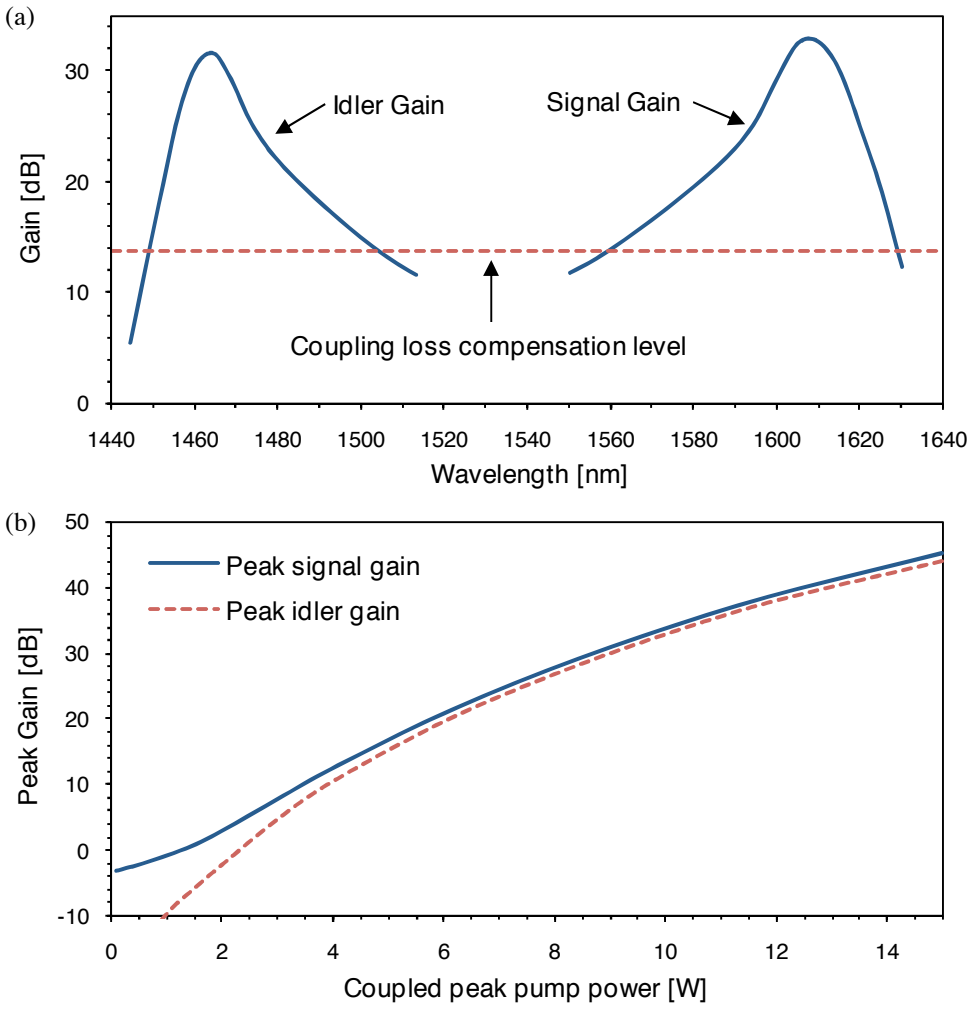


Fig. 6. (a) Signal and idler gain, excluding coupling losses, versus wavelength simulated using same parameters as those used in Fig. 5(b). The horizontal dashed line denotes the level of gain necessary to compensate for coupling losses. (b) Peak signal and idler gain as a function of the pump input peak power, simulated using the same parameters.

based OPAs using similar peak powers, which show strong saturation at gain levels well below that necessary to compensate for the coupling and propagation losses [11].

Despite the large coupling loss of 6.9 dB per facet, we are able to observe a large net-gain. Improvements in fabrication and coupling methods can reduce this loss and increase the power in the output signal and idler. The use of inverse tapers in silicon nanowires has resulted in as little as 0.8 dB of loss per facet [27]. With the use of such devices, the net gain in our chalcogenide waveguides could be increased to ~30 dB.

The peak pump power used in this experiment is significantly larger than the powers used in typical communication systems. However, because the nonlinear phase that drives the FWM process is proportional to $\gamma P_p L$, where $L$ is the device length, the same phase can be applied with reduced $P_p$ using either (or both) increased $\gamma$ or $L$. We are currently researching both of these possibilities through a reduced effective area, which increases $\gamma$, and the use of serpentine (illustrated in Fig. 1) or 'racetrack' waveguides, which increase $L$ without a significant increase in the device footprint. Simulations using FemSIM™ indicate that bending losses should be negligible at the planned bend radius of 50 mm, and experiments in

#103490 - $15.00 USD Received 31 Oct 2008; revised 20 Nov 2008; accepted 21 Nov 2008; published 24 Nov 2008

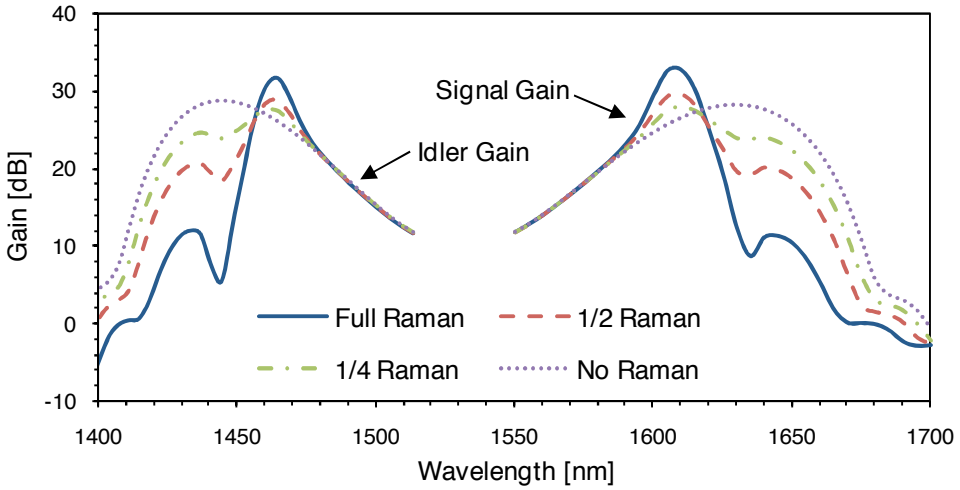


Fig. 7. Simulation of signal and idler gain with decreasing fractional contribution of delayed Raman response.

similar serpentine waveguides support this [22, 28]. This experiment also utilized low average powers (low duty cycle pulses), which is necessary given the average power handling characteristics of chalcogenide glasses. Using the afore-mentioned improvements to reduce peak power, future experiments can be done at similar average powers but at much higher duty cycles (e.g. demonstrations of high bit-rate telecom functionalities) due to the reduced peak power requirements.

The enhancement due to Raman gain can be seen in the cross-phase modulation (XPM) sidebands on the CW signal for wavelength between 1600 and 1620 nm. For the dispersion of the $As_2S_3$ waveguide and pump power used in the experiment, the FWM gain peak occurs within the Raman gain spectrum, further enhancing the parametric amplification. To observe this enhancement directly, Fig. 7 shows simulated gain spectra for decreasing $f_R$, i.e. reducing the contribution of the delayed Raman response. As expected, Raman scattering is responsible for the peak in the gain spectra at the frequency offset corresponding to the peak in the imaginary part of complex Raman susceptibility. However dispersion in the real part of Raman susceptibility causes an additional phase mismatch which affects the phase matching necessary for FWM. By decreasing $f_R$, the additional Raman phase shift is reduced, and the expected FWM gain spectrum is recovered. Thus, Raman scattering has increased the peak gain of the experiment, but has also reduced the bandwidth by impairing the FWM phase matching beyond the Raman gain peak. The theory behind this is outlined by Hsieh et al. and experimentally verified for silica dispersion-shifted fiber [29].

By engineering the dispersion of a highly nonlinear $As_2S_3$ waveguide, we have achieved the first observation of net-gain from parametric amplification in a high-index planar waveguide. We report a peak gain more than +30 dB, which is comparable to the gain expected from a silica fiber OPA or even a commercial EDFA. The net-gain of the device, including all coupling losses, remains greater than +16 dB and represents the first observation of net-gain in a planar waveguide OPA. The bandwidth of the parametric gain is 180 nm, spanning multiple communication bands and double the bandwidth previously demonstrated in silicon waveguides. These preliminary results emphasize the potential of chalcogenide glasses for use in integrated optical devices on a chip for nonlinear signal processing.

**Acknowledgments**

This work was produced with the assistance of the Australian Research Council (ARC). The Centre for Ultrahigh-bandwidth Devices for Optical Systems (CUDOS) is an ARC Centre of Excellence.

#103490 - $15.00 USD Received 31 Oct 2008; revised 20 Nov 2008; accepted 21 Nov 2008; published 24 Nov 2008